

# Increasing Minimum Operating Voltage ( $V_{DDmin}$ ) with Number of CMOS Logic Gates and Experimental Verification with up to 1Mega-Stage Ring Oscillators

Taro Niiyama, Zhe Piao, Koichi Ishida, \*Masami Murakata, Makoto Takamiya, and Takayasu Sakurai

University of Tokyo, 4-6-1 Komaba, Meguro-ku, Tokyo, Japan, 153-8505

\*Semiconductor Technology Academic Research Center (STARC), Japan

## ABSTRACT

In order to explore the feasibility of the large scale subthreshold logic circuits and to clarify the lower limit of supply voltage ( $V_{DD}$ ) for logic circuits, the dependence of minimum operating voltage ( $V_{DDmin}$ ) of CMOS logic gates on the number of stages, gate types and gate width is systematically measured with 90-nm CMOS ring oscillators (RO's). The measured average  $V_{DDmin}$  of inverter RO's increased from 90 mV to 343 mV when the number of RO stages increased from 11 to 1Mega, which indicates the difficulty of the  $V_{DD}$  scaling in the large scale subthreshold logic circuits. The dependence of  $V_{DDmin}$  on the number of stages is calculated with the subthreshold current model with random threshold voltage ( $V_{TH}$ ) variations and compared with the measured results, which confirm the tendency of the measurement.

## Categories and Subject Descriptors

B.7.0 [Integrated Circuits]: General

## General Terms

Measurement, Performance, Design, Reliability, Experimentation.

## Keywords

Minimum operating voltage, subthreshold, logic, variations

## 1. INTRODUCTION

Very low voltage operation of VLSI's is effective in reducing both dynamic and leakage power and the maximum energy efficiency is achieved at low  $V_{DD}$  (e.g. 320mV [1]). Thus many works have been carried out on the subthreshold operation of logic circuits [1, 3-6] and SRAM's [2], where  $V_{DD}$  is less than  $V_{TH}$  of transistors. However, the number of transistors of the previously reported subthreshold circuits is small (e.g. 70k transistor logic circuits at  $V_{DD}$  of 230mV [1], a 32kbit SRAM at  $V_{DD}$  of 160mV [2], and a 1000 stage inverter chain at  $V_{DD}$  of 60mV [5]), and the possibility of the mega gate scale subthreshold circuits is not clear.

Permission to make digital or hard copies of all or part of this work for personal or classroom use is granted without fee provided that copies are not made or distributed for profit or commercial advantage and that copies bear this notice and the full citation on the first page. To copy otherwise, or republish, to post on servers or to redistribute to lists, requires prior specific permission and/or a fee.

ISLPED '08, August 11-13, 2008, Bangalore, India.

Copyright 2008 ACM 978-1-60558-109-5/08/08...\$5.00.

$V_{DDmin}$  is the minimum power supply voltage when the circuits operates without function errors. RO's are useful  $V_{DDmin}$  detectors [7], because RO's stop oscillation when the first function error in the logic circuits happens. Figure 1 shows simulated waveform of 5-stage CMOS inverter RO.  $V_{DD}$  is varied from 0.2V to 0V. At  $V_{DDmin}$  of 50mV, RO stops oscillation. In order to emulate the recent SoC's, the mega stage scale RO's are required, because the recent SoC's have 10M-100M logic gates. With the technology scaling and the increased number of transistors on a chip,  $V_{DDmin}$  will increase, because the more gates there are, the more likely it is that the worst-case condition will occur, and thus a higher  $V_{DD}$  will be required. However, the systematic measurements of the  $V_{DDmin}$  of the subthreshold logic circuits made with scaled devices have not been reported yet.

This paper reports the systematically measured dependence of  $V_{DDmin}$  of CMOS logic gates on the number of stages, gate types and gate width with 90-nm CMOS RO's for the first time in order to explore the feasibility of the large scale subthreshold logic circuits and to clarify the lower limit of  $V_{DD}$  for logic circuits.

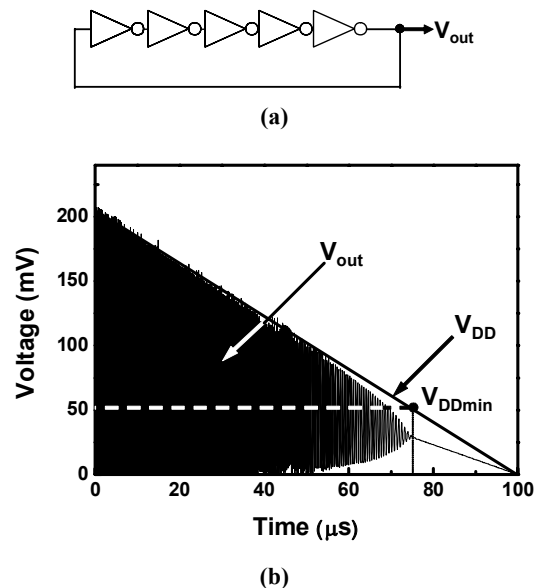


Figure 1. Simulated waveform of 5-stage CMOS inverter RO. Definition of  $V_{DDmin}$  is shown.

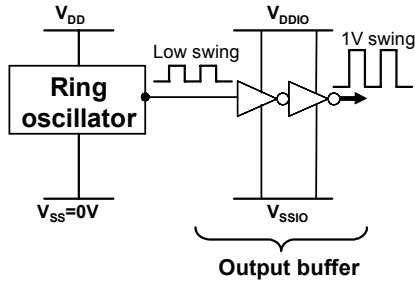


Figure 2. Proposed RO circuits to enable the  $V_{DDmin}$  measurement.

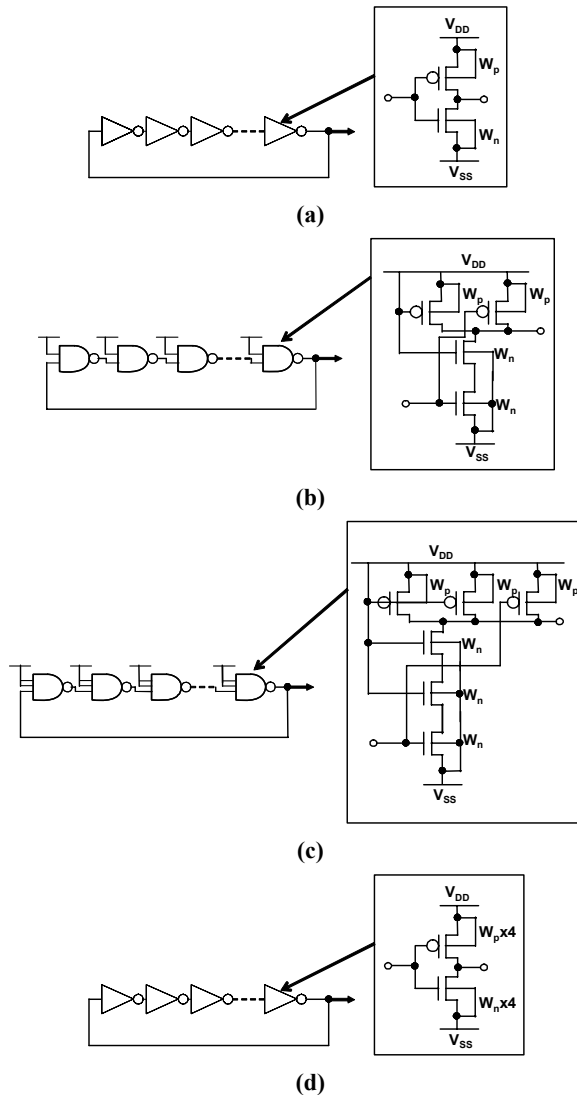


Figure 3. Fabricated RO circuits with varied number of stages. (a) Inverter RO, (b) 2NAND RO, (c) 3NAND RO, (d) x4 inverter RO.

Section 2 presents the design of CMOS RO's for  $V_{DDmin}$  measurement and the measured  $V_{DDmin}$ . Section 3 presents the analysis of the origin of  $V_{DDmin}$  with SPICE and MATLAB to explain the measured results.

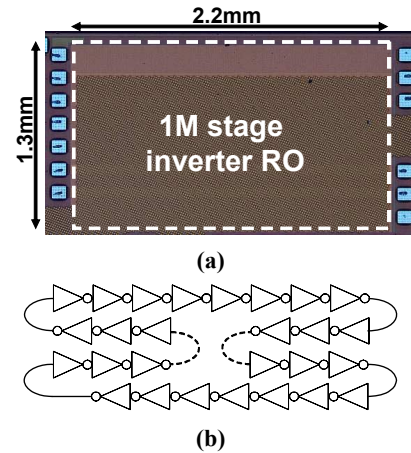


Figure 4. (a) Micrograph of a 1M-stage inverter RO. (b) Layout style of RO's.

## 2. MEASURED $V_{DDmin}$ of 90-nm CMOS RO's

### 2.1 Design of CMOS RO's for $V_{DDmin}$

#### Measurement

Figure 2 shows the schematic of the proposed RO circuits to enable the  $V_{DDmin}$  measurement. The low swing output of RO is amplified to 1-V swing by the output buffer, because both  $V_{DD}$  and  $V_{SS}$  of RO are separated from the  $V_{DDIO}$  and  $V_{SSIO}$  of the output buffer by the triple well and  $V_{SS}$  is manually tuned to the optimum input level for the output buffer in the measurement.  $V_{DDmin}$  is defined as the supply voltage ( $= V_{DD} - V_{SS}$ ) when the RO's stop oscillation and no voltage transitions from the output buffer are observed, which corresponds to the function errors in logic LSI's.

Figure 3 shows the schematic of fabricated RO circuits with varied number of stages. RO's include three different logic gates (inverter, 2NAND and 3NAND) and two inverters with different gate width. The standard primitive cells are used for the logic gates and the P/N ratio was not optimized for the minimum  $V_{DD}$  operation. The gate length is the minimum in 90 nm CMOS process. The gate width of nMOS ( $W_n$ ) and pMOS ( $W_p$ ) are  $0.54\mu\text{m}$  and  $0.82\mu\text{m}$  respectively. RO's were fabricated with 1 V 90 nm CMOS process in three different lots. The first lot includes inverter RO's from 11-stage to 1Mega-stage to investigate the dependence of  $V_{DDmin}$  on the number of stages. The second lot includes inverter RO's, 2NAND RO's and 3NAND RO's to investigate the gate type dependence. The third lot includes inverter RO's and x4 inverter RO's to investigate the gate width dependence.

Figure 4(a) shows the micrograph of a 1Mega-stage inverter RO in 90 nm CMOS. The core area is  $2.2\text{mm} \times 1.3\text{mm}$ . Figure 4(b) shows the layout style of RO's. In order to remove the effect of the global variation on RO's, the interconnect length between the

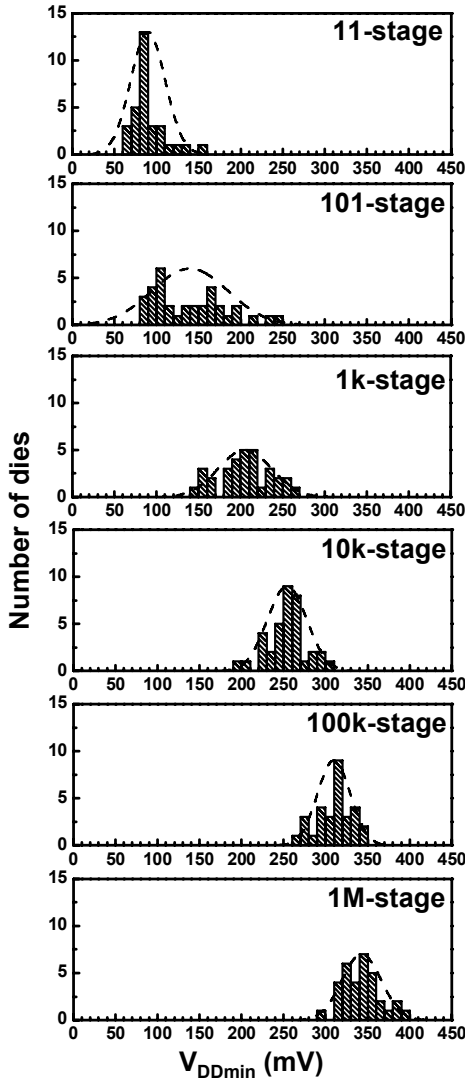


Figure 5. Die-to-die distribution of  $V_{DDmin}$  of inverter RO's with different number of stages from 11-stage to 1M-stage.

inverters is as short as possible and the maximum interconnect length in the 1Mega-stage inverter RO is  $3.5\mu\text{m}$ .

## 2.2 Dependence of $V_{DDmin}$ on Number of Stages

Figure 5 shows the measured die-to-die distribution of  $V_{DDmin}$  of inverter RO's with different number of stages from 11-stage to 1M-stage. Figure 6 shows the measured dependence of the average  $V_{DDmin}$  with  $\pm 1\sigma$  error bar of inverter RO's on the number of stages extracted from Figure 5. As the number of stages is increased, the average  $V_{DDmin}$  increase, because  $V_{DDmin}$  is determined by the worst inverter(s) in each RO. For example, the average  $V_{DDmin}$  increases from 90 mV to 343 mV when the number of RO stages increases from 11 to 1Mega. The 343 mV means above  $V_{TH}$  operation. The results indicate that  $V_{DDmin}$  for logic circuits depends on the scale of the circuits and large scale

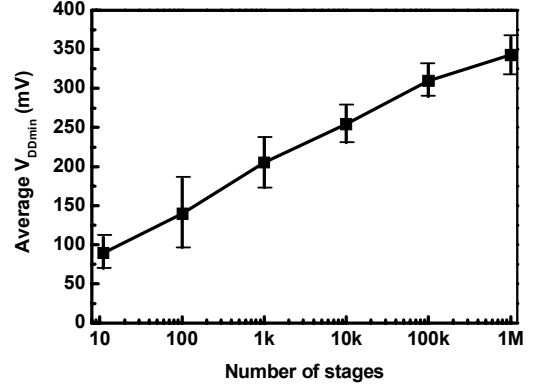


Figure 6. Measured dependence of the average  $V_{DDmin}$  of inverter RO's on the number of stages.

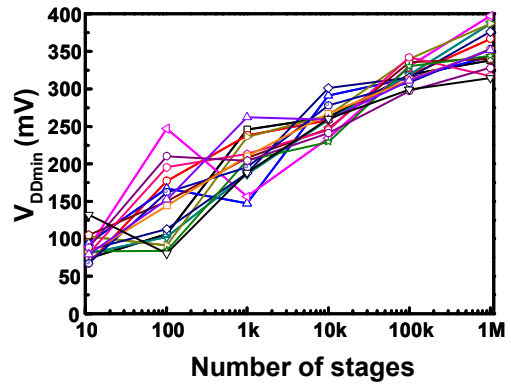


Figure 7. Measured dependence of  $V_{DDmin}$  of inverter RO's on the number of stages for 15 dies.

logic circuits have high  $V_{DDmin}$ . In order to analyze the die-to-die  $V_{DDmin}$  variations, Figure 7 shows the measured dependence of  $V_{DDmin}$  of inverter RO's on the number of stages for 15 dies. The die-to-die  $V_{DDmin}$  variations are not systematic but random.

## 2.3 Dependence of $V_{DDmin}$ on Gate Types

Figure 8 shows the measured dependence of the average  $V_{DDmin}$  of inverter, 2NAND and 3NAND RO's on the number of stages from 11-stage to 1k-stage. The three lines have the similar gradient, but they have different offsets. The gradient is determined by the transistor variations and the offsets are determined by the unbalance between nMOS and pMOS. In this work, 3NAND RO's have the highest average  $V_{DDmin}$ , because both  $W_n$  and  $W_p$  are the same for the inverter, 2NAND and 3NAND RO's as shown Figures 3(a)-(c) and the 3NAND RO's have the largest unbalance between nMOS and pMOS. The unbalance, however, can be solved by tuning  $W_p/W_n$  ratio.

## 2.4 Dependence of $V_{DDmin}$ on Gate Width

Die-to-die distribution of  $V_{DDmin}$  of inverter RO's and x4 inverter RO's with different number of stages from 11-stage to 1Mega-stage is measured. The lowest  $V_{DDmin}$  was 58 mV for the 11-stage RO's. Figure 9 shows the measured dependence of the average  $V_{DDmin}$  of inverter and x4 inverter RO's on the number of stages. The two lines have the similar offset, but they have different gradients. In theory, the gradient of the x4 inverter RO's is half of

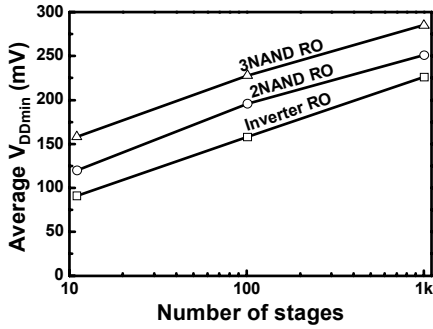


Figure 8. Measured dependence of the average  $V_{DDmin}$  of inverter, 2NAND and 3NAND RO's on the number of stages.

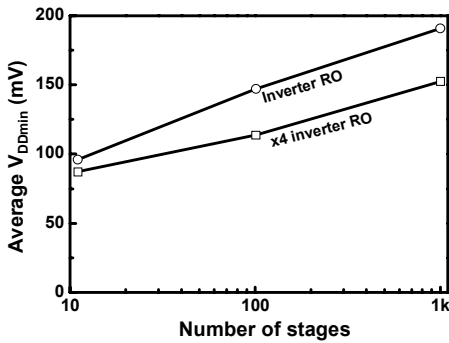


Figure 9. Measured dependence of the average  $V_{DDmin}$  of inverter and x4 inverter RO's on the number of stages.

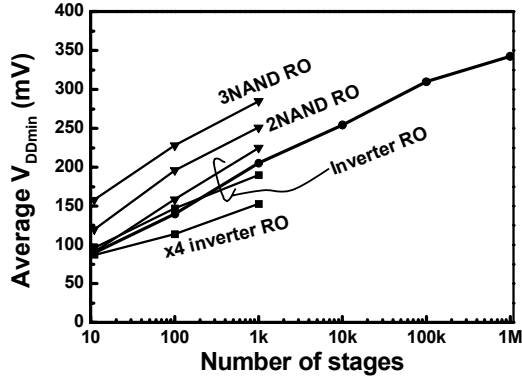


Figure 10. Summary the measured dependence of the average  $V_{DDmin}$  of all RO's lots on the number of stages.

that of the inverter RO's, because the x4 gate width halves the  $V_{TH}$  variations. The measured gradient of the x4 inverter RO's, however, is 70% of that of the inverter RO's.

## 2.5 Summary of $V_{DDmin}$ Measurement

Figure 10 summarizes the measured dependence of the average  $V_{DDmin}$  of all RO's lots on the number of stages extracted from Figures 6, 8 and 9. The three lines of the inverter RO's show the measured average  $V_{DDmin}$  in three different lots. While increasing the number of stages and the number of stacked transistors increases  $V_{DDmin}$ , the wide gate width decreases  $V_{DDmin}$ .

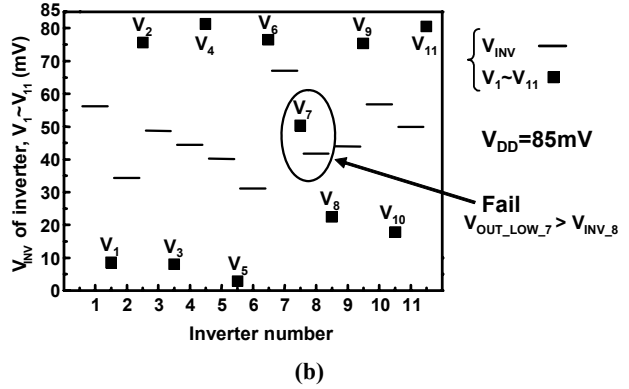
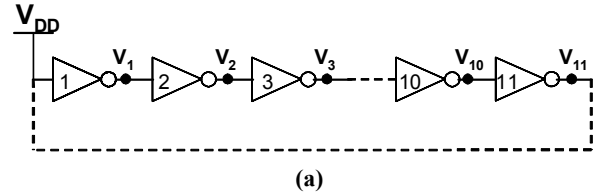


Figure 11. (a) Simulated 11-stage inverter chain where each transistor has random  $V_{TH}$ . (b) Node voltages ( $V_1-V_{11}$ ) and inversion voltages ( $V_{INV}$ 's) of the inverters.

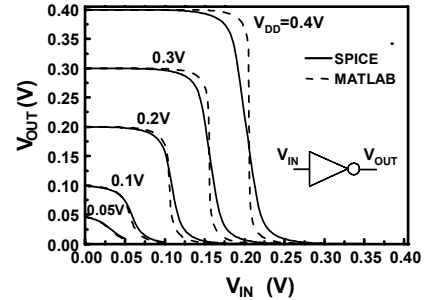


Figure 12. Comparison of the inverter characteristic of SPICE and Matlab.

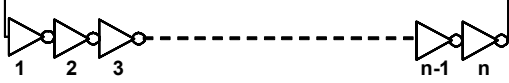
## 3. ANALYSIS OF $V_{DDmin}$

### 3.1 Analysis of $V_{DDmin}$ with SPICE

The origin of the  $V_{DDmin}$  is analyzed with Monte Carlo SPICE simulations. Figure 11(a) shows the schematic of the simulated 11-stage RO's where each transistor has random  $V_{TH}$ . The inverter chain with the input of  $V_{DD}$  is simulated. Figure 11(b) shows the node voltages ( $V_1-V_{11}$ ) and the inversion voltages ( $V_{INV}$ 's) of the inverters. Normally, the logical low of  $V_1-V_{11}$  is lower than  $V_{INV}$  and the logical high of  $V_1-V_{11}$  is higher than  $V_{INV}$ . The inverter chain, however, has a function error at #7 and #8 inverter, because #7 inverter has slow nMOS and fast pMOS,  $V_{INV}$  of #7 inverter is high, and the logical low of  $V_7$  ( $V_{OUT\_LOW\_7}$ ) is higher than  $V_{INV}$  of #8 inverter. The function error stops the RO oscillation.

### 3.2 Comparison of Measured and Calculated $V_{DDmin}$

In order to investigate the increasing average  $V_{DDmin}$  with the number of stages, the simulations of  $V_{DDmin}$  from 11-stage to 1Mega-stage RO's are required. However, the simulations of



$n = \text{Odd number}$

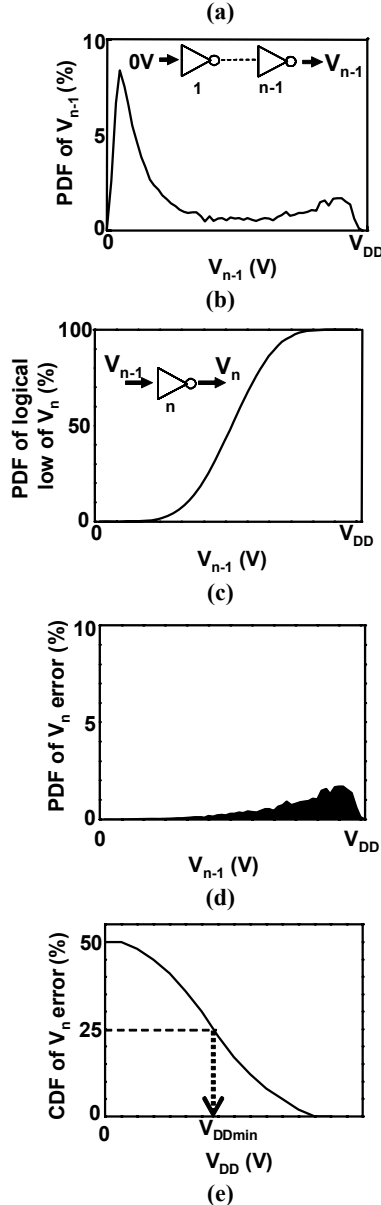


**Figure 13. Calculation steps of  $V_{DDmin}$  of n-stage RO. (a) Calculated n-stage inverters. (b) PDF of the output of the (n-1)-stage inverter chain with the input of 0V. (c) PDF of the logical low (=error) of  $V_n$ . (d) PDF of  $V_n$  error. (e) CDF of  $V_n$  error.**

$V_{DDmin}$  of up to 1Mega-stage RO's with Monte Carlo SPICE take too long time and are not practical. Therefore,  $V_{DDmin}$  is calculated with the subthreshold current model with random  $V_{TH}$  variations and compared with the measured results. Equation (1) shows the drain current model of MOSFET in the subthreshold region.

$$I_D = C_1 e^{C_2(V_{GS}-V_{TH})} (1 - e^{-C_3 V_{DS}}) \quad (1)$$

$I_D$  is the drain current,  $V_{GS}$  is the gate-to-source voltage and  $V_{DS}$  is the drain-to-source voltage.  $C_1$ ,  $C_2$  and  $C_3$  are constants. In the CMOS inverter, the input-output characteristic of the inverter is derived by equating  $I_D$  of nMOS and pMOS. Figure 12 shows the comparison of the inverter characteristic of SPICE and the calculation with Equation (1). MATLAB is used for the calculation.  $V_{DD}$  is varied from 50mV to 0.4V. The calculation is verified by comparing with SPICE. Below  $V_{DD}$  of 0.2V, the calculation error is small. In contrast, Above  $V_{DD}$  of 0.3V, the calculation error is large, because the calculation includes only the diffusion current (= subthreshold current) and neglects the drift current (= strong inversion current).

Figure 13 shows the calculation steps of  $V_{DDmin}$  of a n-stage RO, where n is an odd number. The transistors in the RO have random  $V_{TH}$  variations. First, the probability density function (PDF) of the output ( $V_{n-1}$ ) of the (n-1)-stage inverter chain with the input of 0V is calculated by cascading the (n-1)-stage inverters as shown in Figure 13(b). Though the correct  $V_{n-1}$  is low, Figure 13(b) shows some incorrect high  $V_{n-1}$  due to the function error. Then, the PDF of the logical low (=error) of  $V_n$  by integrating the  $V_{INV}$  distribution is as shown in Figure 13(c). Figure 13(d) shows PDF of  $V_n$  error derived by multiplying Figure 13(b) by Figure 13(c). Finally, Figure 13(e) shows the cumulative distribution function (CDF) of  $V_n$  error derived by integrating Figure 13(d). Strictly speaking, CDF of  $V_n$  error of the n-stage inverter chain with the input of  $V_{DD}$  should also be calculated and added to Figure 13(e). However, the inputs of 0V or  $V_{DD}$  are symmetry. Therefore,  $V_{DDmin}$  is defined as  $V_{DD}$  when CDF of  $V_n$  error equals to 25% as shown in Figure 13(e).

Table I shows the 4 sets of  $\sigma V_{TH}$ 's of nMOS and pMOS used in the calculation.  $\sigma V_{TH}$ 's are originally determined by the Pelgrom plot, however,  $\sigma V_{TH}$ 's are varied to fit the measured results. Figure 14 shows the comparison of measured and calculated dependence of the average  $V_{DDmin}$  of inverter RO's on the number of stages. The measured x4 inverter RO's are also plotted. The calculation shows the expected increasing gradients and offsets with increased  $\sigma V_{TH}$ , which confirm the tendency of the measurement. The two reasons for the quantitative error between the measurement and MATLAB are; (1) Only  $V_{TH}$  variations are considered in the calculation and no other variations are not considered. (2) The inverter characteristic error increases with the increased  $V_{DD}$  as shown in Figure 12, because the model includes only the subthreshold current and neglects the strong inversion current.

Finally, the reason why the average  $V_{DDmin}$  increases with the number of RO stages is discussed. Generally, the largest value distributions  $f_{max}(x,n)$  of n samples which have Gaussian distribution  $f(x)$  are shown in Figure 15.

$$f(x) = \frac{1}{\sqrt{2\sigma}} e^{-\frac{(x-\bar{x})^2}{2\sigma^2}} \quad (2)$$

$$f_{max}(x,n) = \frac{d}{dx} \left\{ \left( \int_{-\infty}^x \frac{1}{\sqrt{2\sigma}} e^{-\frac{(y-\bar{x})^2}{2\sigma^2}} dy \right)^n \right\} \quad (3)$$

Table I. Several sets of  $\sigma V_{TH}$ 's of nMOS and pMOS used in the calculation.

Name	$\sigma V_{TH}$ (mV)		Remarks
	nMOS	pMOS	
Sim075	25.8	22.5	x0.75
Sim100	34.4	30.0	x1
Sim125	43.0	37.5	x1.25
Sim150	51.6	45.0	x1.5

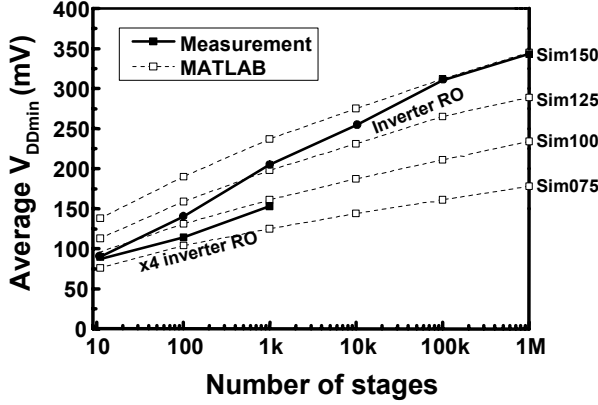


Figure 14. Comparison of measured and calculated dependence of the average  $V_{DDmin}$  of inverter RO's on the number of stages.

$\bar{x}$  is the average of  $x$  and  $\sigma$  is the standard variation of  $x$ . The  $x$  value ( $\bar{x}_{max}$ ) where  $f_{max}(x,n)$  has its peak is approximated as

$$\bar{x}_{max} \cong \bar{x} + 2\sqrt{\log_{10} n} \sigma \quad (4)$$

Figure 16 shows the  $n$  dependence of  $\bar{x}_{max}$ , and compares the exact and approximated results. Equation (4) intuitively explains the reason why the average  $V_{DDmin}$  increases with the number of RO stages. The calculated dependence in Figure 14 is also approximated by Equation (4) and the error was negligible small.

## 4. CONCLUSIONS

The minimum operating voltage ( $V_{DDmin}$ ) of 90-nm CMOS logic gates has been investigated with the ring oscillators. The measured average  $V_{DDmin}$  of inverter RO's increased from 90 mV to 343 mV when the number of RO stages increased from 11 to 1Mega, which indicates the difficulty of the  $V_{DD}$  scaling in the large scale subthreshold logic circuits. While increasing the number of stages and the number of stacked transistors increases  $V_{DDmin}$ , the wide gate width decreases  $V_{DDmin}$ . The dependence of  $V_{DDmin}$  on the number of stages is calculated with the subthreshold current model with random threshold voltage variations, which confirm the tendency of the measurement.

## 5. ACKNOWLEDGMENTS

This work is partially supported by STARC. The VLSI chips were fabricated through the chip fabrication program of VLSI Design and Education Center (VDEC), the University of Tokyo, with the collaboration by STARC, Fujitsu Limited, Matsushita Electric Industrial Company Limited., NEC Electronics Corporation, Renesas Technology Corporation, and Toshiba Corporation.

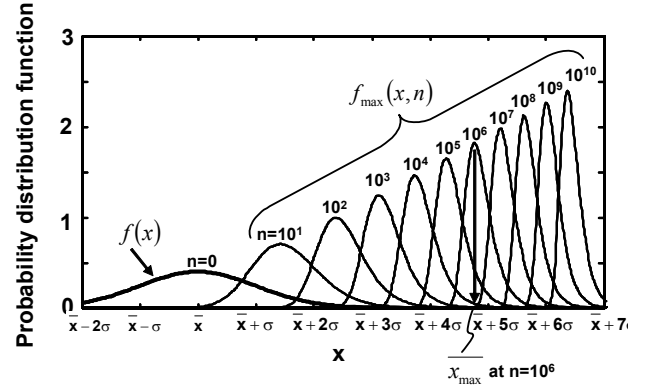


Figure 15. The largest value distributions  $f_{max}(x,n)$  of  $n$  samples which have Gaussian distribution  $f(x)$ .

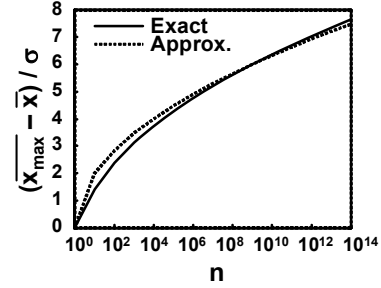


Figure 16. Comparison of exact and approximated results in  $n$  dependence of  $\bar{x}_{max}$ .

## 6. REFERENCES

- [1] H. Kaul, M. Anders, S. Mathew, S. Hsu, A. Agarwal, R. Krishnamurthy, and S. Borkar, "A 320mV 56μW 411GOPS/Watt ultra-low voltage motion estimation accelerator in 65nm CMOS," IEEE International Solid-State Circuits Conference, pp. 316-317, Feb. 2008.
- [2] I. Chang, J. Kim, S. Park, and K. Roy, "A 32kb 10T Subthreshold SRAM Array with Bit-Interleaving and Differential Read Scheme in 90nm CMOS," IEEE International Solid-State Circuits Conference, pp. 388-389, Feb. 2008.
- [3] B. Calhoun, and A. Chandrakasan, "Ultra-dynamic voltage scaling (UDVS) using sub-threshold operation and local voltage dithering," IEEE Journal of Solid-State Circuits, Vol. 41, No. 1, pp. 238-245, Jan. 2006.
- [4] S. Hanson, B. Zhai, M. Seok, B. Cline, K. Zhou, M. Singhal, M. Minuth, J. Olson, L. Nazhan-dali, T. Austin, D. Sylvester, and D. Blaauw, "Performance and variability optimization strategies in a sub-200mV, 3.5pJ/inst, 11nW subthreshold processor," IEEE Symposium on VLSI Circuits, pp. 152-153, June 2007.
- [5] M. Hwang, A. Raychowdhury, K. Kim, and K. Roy, "A 85mV 40nW process-tolerant subthreshold 8x8 FIR filter in 130nm technology," IEEE Symposium on VLSI Circuits, pp. 154-155, June 2007.
- [6] J. Kwong and A. Chandrakasan, "Variation-Driven Device Sizing for Minimum Energy Sub-threshold Circuits," International Symposium on Low Power Electronics and Design, pp. 8-13, Oct. 2006.
- [7] T. Niiyama, P. Zhe, K. Ishida, M. Murakata, M. Takamiya, and T. Sakurai, "Dependence of Minimum Operating Voltage ( $V_{DDmin}$ ) on Block Size of 90-nm CMOS Ring Oscillators and Its Implications in Low Power DFM," IEEE International Symposium on Quality Electronic Design, pp. 133-136, March 2008.